

Generation, Stabilization, and Amplification of Subpicosecond Pulses*

S. R. Rotman, C. Roxlo, D. Bebelaar*, T. K. Yee, and M. M. Salour

Massachusetts Institute of Technology
Department of Electrical Engineering and Computer Science
Research Laboratory of Electronics
Cambridge, MA 02139, USA

Received 12 November 1981/Accepted 26 March 1982

Abstract. A sync-pumped cw dye laser system has been used to produce subpicosecond pulses. Pulses as short as 0.7 ps, assuming a single-sided exponential pulse shape, were observed. A set of experiments was performed to investigate the origin and effects of noise in the sync-pumped system. A digital and an analog feedback loop have been designed to optimize the pulse width. The noise has been lowered by 10 dB for frequencies up to 10 kHz; long-term drift is also controlled by this method. A four-stage dye laser amplifier, pumped by a Nd:YAG laser which operates at a 10-Hz repetition rate, is synchronized electronically to the dye-laser picosecond pulses. A gain of 3×10^6 has been achieved.

PACS: 07.60, 07.65, 42.60

Short light pulses have been used for many years in the study of physical phenomena [1]. Their extension to the picosecond and subpicosecond range has recently allowed the observation of previously unresolved processes [2, 3] in physics, chemistry, and biology. One method of generating picosecond pulses for time-resolved spectroscopy at megahertz repetition rates is the synchronously pumped cw dye laser.

Ever since pulses a few picoseconds long were first achieved in this manner by Chan and Sari [4], considerable effort has been directed to obtain pulses as short as those from a passively mode-locked cw dye laser, which can generate pulses down to 90 femtoseconds [5]. The shortest pulses generated by synchronously pumped cw dye lasers have been just below 1 ps, either by pumping in tandem [6] or directly [7] with pulses of 50 ps or shorter. The choice of the spectral bandwidth [8, 9] and output coupler [10] of the dye laser is important to obtain short pulses, but

the most crucial parameter is the timing of the pump pulses relative to the pulse circulating in the dye-laser cavity. The sensitivity in matching the pump-pulse repetition rate to the round-trip time in the dye laser [10, 11] is on the order of one part per million for the generation of 1-ps pulses (about 1 μm at a cavity length of 1.8 m).

To date, efforts have been directed towards eliminating noise which affects the critical parameters in sync-pumping: the oscillator driving the mode locker in the pump laser which determines the pump-pulse repetition rate and the cavity length of the dye laser which controls the round-trip time of the dye-laser pulse. Another approach is to detect and correct for any perturbation by adjusting one of the critical parameters. This method of active feedback has been used in single-frequency dye lasers in the past with great success, giving a smaller spectral bandwidth than that obtained with passive stabilization techniques.

This paper describes a sync-pumped cw dye laser using active feedback to stabilize the pulse width. For experiments requiring high peak power the pulses are amplified to gigawatt peak powers at the expense of a lower repetition rate.

* This work was supported by the Joint Services Electronics Program

** Present address: Laboratory for Physical Chemistry, University of Amsterdam, The Netherlands

1. Experimental Setup

Two Rhodamine 6G dye lasers were synchronously pumped by an Ar⁺ laser. The Ar⁺ laser produced a train of light pulses of approximately 100-ps duration at a repetition rate of 82 MHz and an average power of roughly 1/2 w for each dye laser, using an output coupler of 30% transmission. A Spectra-Physics Model 451 oscillator and a Hewlett-Packard Model HP 8640B signal generator were alternately used to drive the piezo-electric transducer which sets up the acoustic standing waves in the prism in the Ar⁺ laser cavity at a frequency of 40.8675 MHz. The first dye laser contains a wedge in its cavity to narrow the spectral bandwidth of the dye laser and to allow for wavelength tuning [10]. The output mirror is a standard Spectra-Physics output coupler with 30% transmission at 575 nm and 12% transmission at 610 nm.

The width of a pulse increases as its bandwidth decreases [8]. To achieve as short a pulse as possible at maximum power output, the second dye laser was operated without any bandwidth-limiting elements and with an output mirror having a 30% transmission, constant over the wavelength range of Rhodamine 6G.

The dye lasers' pulse widths were measured on an intensity autocorrelator, similar to that used by Fork [12], by observing second-harmonic generation (SHG) in a KDP crystal. The measured pulse width of the first dye laser increases with increasing wavelength up to 630 nm.

The second dye laser was found to give a pulse of 0.7 ps duration at a wavelength of approximately 590 nm. The higher output coupling is necessary to produce this pulse width, but higher pump power was required to reach the threshold. An incremental efficiency of 20% was obtained from each laser at their optimum settings.

The length of the dye laser must be adjusted to within microns in the case of active mode locking. The cavity of the first dye laser, 1.8 m in length, was controlled by a manually adjustable quartz rod. The cavity length of the second dye laser was automatically set by a minicomputer (DEC MINC System) which controlled the position of a Klinger translation stage on which its output coupler was mounted.

2. Noise in a Synchronously Pumped Dye-Laser System

Pulse-width fluctuations of the sync-pumped cw dye laser are caused by changes in the pump-pulse amplitude, width, and timing. These can originate from electrical noise in the oscillator which provides the

signal for the acousto-optic modulator. Further sources are variations in the electrical discharge in the Ar⁺ laser caused by the power supply, mechanical noise in the Ar⁺ laser resonator, plasma instabilities, etc. Noise is also introduced by changes in the optical cavity length of the dye laser, mainly caused by temperature changes, atmospheric pressure fluctuations, dye jet fluctuations, etc.

The pulse width and its variations are, in general, measured with an autocorrelator [12]. This is, however, a relatively slow method since a mechanical motion of the scanning arm is involved. Pulse-width fluctuations can also be detected in a much faster way by measuring the SHG output after focusing the output pulses from the dye laser in a frequency-doubling crystal. The resulting second-harmonic power follows the relation [13]

$$P_{SH} \propto \frac{(P_F)^2}{\tau} \quad (1)$$

where P_{SH} is the average power of the second harmonic [also referred to as SHG (second-harmonic generation)], τ is the pulse width, and P_F is the average power of the visible radiation at the fundamental optical frequency. By differentiating (1), we find that, for small changes in P_F and P_{SH} ,

$$d\tau \propto \frac{2dP_F}{P_F} - \frac{dP_{SH}}{P_{SH}} \quad (2)$$

where dP_F , dP_{SH} , and τ are the incremental changes of P_F , P_{SH} , and τ , respectively. Thus $2dP_F/P_F - dP_{SH}/P_{SH}$ is a measure of the variation in pulse width.

As mentioned earlier, the length of the dye-laser cavity and the repetition rate of the mode-locked Ar⁺ laser must be carefully matched to assure the best pulse. A change of only one part in 10⁵ of the oscillator frequency causes a large variation in the second-harmonic power P_{SH} . However, the visible power P_F changes at most by only 10%. Figure 1 exhibits the SHG power versus driver frequency for the second dye laser. The frequency setting for the shortest pulse [10] is not that for maximum P_{SH} , but occurs at a frequency approximately 40 Hz less. Changes of as little as 10 Hz (which corresponds to a change in length of $\approx 0.5 \mu\text{m}$ in the 1.8-m cavity) produce noticeable changes in the pulse shape, as observed on the auto-correlator. The setting for maximum P_{SH} does not coincide completely with shortest pulse setting (P_F being almost constant) because a very small portion of the fundamental power is contained in the wings of the pulse, as was verified with the auto-correlator.

The frequency spectrum of the noise at several points in the sync-pumped dye laser was measured using both low-frequency (Tektronics 7L5) and high-frequency

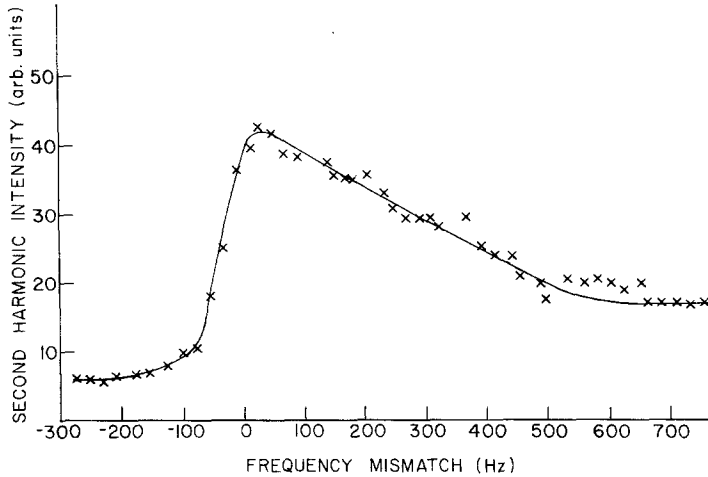


Fig. 1. SHG power output as a function of frequency mismatch for the second dye laser. Zero-frequency mismatch is the frequency of maximum SHG output

(7L13) spectrum analyzers. The Spectra-Physics oscillator is noticeably noisier compared with the Hewlett Packard oscillator; sidebands occur at harmonics spaced at intervals of 500 Hz, which is the frequency of its phase-locked loop. The sidebands (the first one being down by 40 dB) are an indication of a small (~10-Hz swing) FM square-wave modulation of the rf output.

The frequency spectrum of the rf output of the Hewlett-Packard oscillator does not show any sidebands. The FWHM frequency bandwidth is within the resolution limit of the 7L13 spectrum analyzer which is 30 Hz.

Figure 2 compares the noise-frequency spectrum of P_{SH} to that of P_F of the dye laser at the driving frequency giving the shortest pulse. The curves have been normalized such that they would coincide if the fluctuations were caused by amplitude variations. Over 10 dB of the noise can be explained by pulse-width fluctuations. The propagation of the 500-Hz modulation of the Spectra-Physics oscillator through the whole system can also be seen in Fig. 2. The modulation of the oscillator causes large spikes in the dye-laser spectrum at 500-Hz intervals because the modulation manifests itself in jitter of the interarrival time of the Ar^+ pulses. When the Ar^+ laser output is measured with a photodiode and similarly analyzed with the 7L5 spectrum analyzer, the modulation is hardly visible.

Finally, the spectrum of the Ar^+ and the dye laser outputs were measured at frequencies up to the megahertz range. The noise in the Ar^+ intensity was reasonably flat up to frequencies above one megahertz. The noise in the frequency-doubled dye laser output (Fig. 3, using the Hewlett Packard oscillator), however, had a different character with its greatest intensity in a band between 100 and 150 kHz, perhaps caused by fluctuations in the Ar^+ laser. The difference in the two

curves in Fig. 3 shows that about 3 dB of the previously mentioned 10-dB pulse-width fluctuations is caused by the sensitivity of the sync-pumped dye laser to the interarrival time of the pump pulses. Control of this noise is the ultimate goal of any stabilization

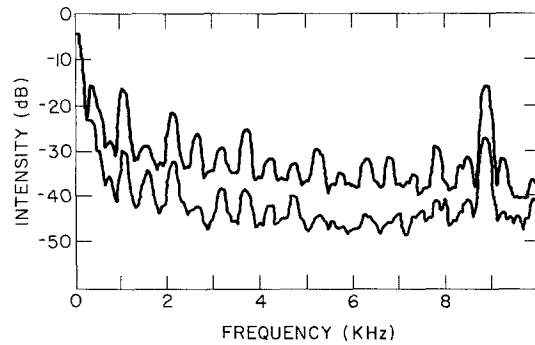


Fig. 2. Frequency spectra of the second-harmonic signal (top trace) and the fundamental signal (bottom trace) from the dye laser at the shortest pulse frequency. A Spectra-Physics oscillator (Model 452) is used. The resolution of the spectrum analyzer is 100 Hz

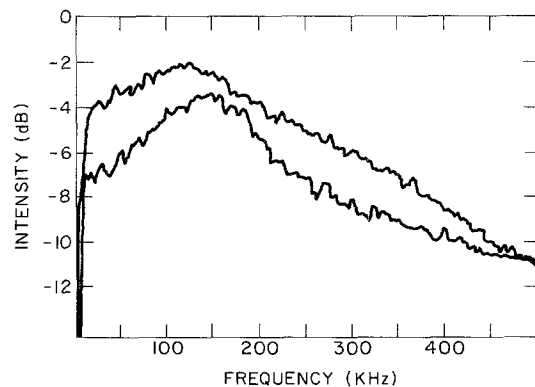


Fig. 3. Frequency spectra of the second-harmonic signal from the dye laser at the frequency of best pulse formation (top trace) and the frequency of maximum second-harmonic power (bottom trace). Resolution of the spectrum analyzer is 3 kHz

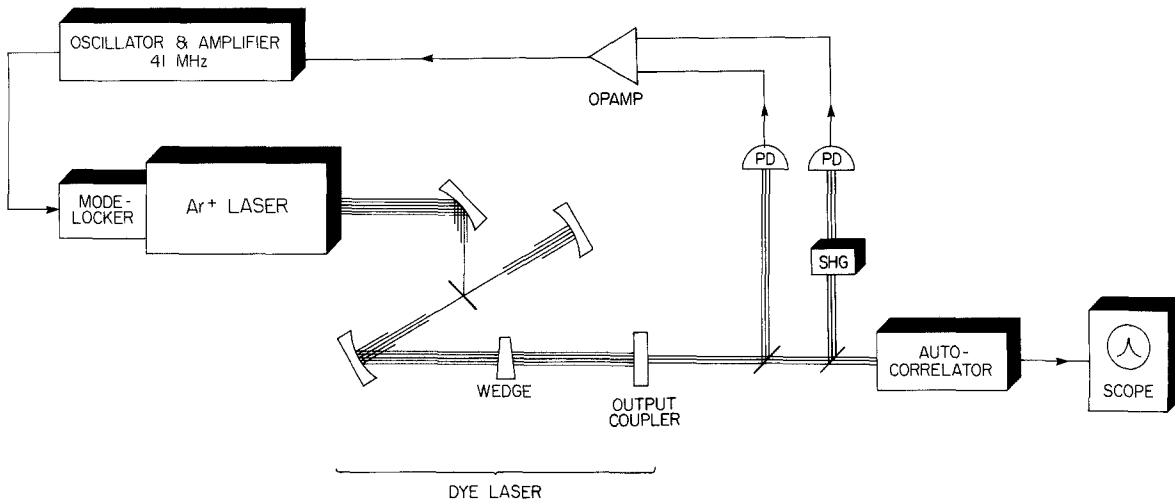


Fig. 4. Schematic of the analog feedback loop

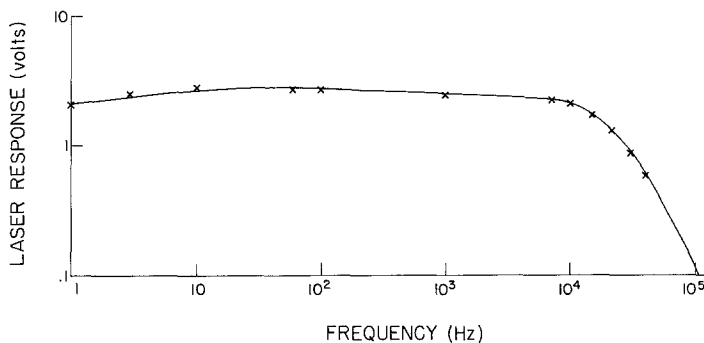


Fig. 5. A graph of the magnitude of the SHG output modulated with a peak-to-peak deviation of 250 Hz as a function of modulation frequency

system. This will require a bandwidth of approximately 150 kHz.

3. Analog and Digital Feedback

Correction of pulse-width fluctuations of the dye laser by active feedback can be accomplished by controlling either the repetition rate of the pumping pulses or the cavity length of the dye laser. The first method has been used here in an analog way; the second method involves a digital minicomputer. If the repetition rate of the Ar⁺ laser pulses is varied by changing the frequency of the mode-lock driver, the Ar⁺ laser pulse shape is hardly affected in a range of about 50 Hz (1 part in 10⁶) during which the dye-laser pulse width is changing dramatically. This was verified by observing the Ar⁺ laser pulse with a fast photodiode-sampling oscilloscope combination. The relative insensitivity of the Ar⁺ laser to the mode-locked frequency allows us to change the oscillator frequency without upsetting the Ar⁺ laser. The fact that the shortest pulse occurs not at the maximum of the SHG curve but at the slope (slightly below the maximum) simplifies the feedback considerably. Fluctuations in the SHG signal around

this operating point can be fed back directly as frequency modulation to the driving oscillator. The advantage of this scheme is its inherent fast response since no mechanical motion is involved.

Our analog loop is schematically shown in Fig. 4. The signal $2\Delta P_F/P_F - \Delta P_{SH}/P_{SH}$ is fed to a differential amplifier (Tektronix 1A7A oscilloscope/plug-in). This amplifier provides the capability to vary both the gain constant of the loop and the low- and high-frequency rolloff points. The signal was then sent to the HP 8640B oscillator to frequency-modulate its carrier frequency.

In this analog scheme the frequency response of the detection of the pulse-width fluctuations and the frequency modulation of the HP 8640B oscillator can extend into the MHz range. However, the response of the acousto-optic mode-locking prism in the Ar⁺ laser cavity is much slower. A frequency response of 10 kHz was determined by deliberately modulating the frequency of the HP 8640B signal generator and measuring the modulation of the SHG output (Fig. 5) and its phase relation to the driving frequency.

Figure 6 shows the frequency response of the dye laser with closed feedback loop for several values of high cutoff frequencies. The low-frequency cutoff point was

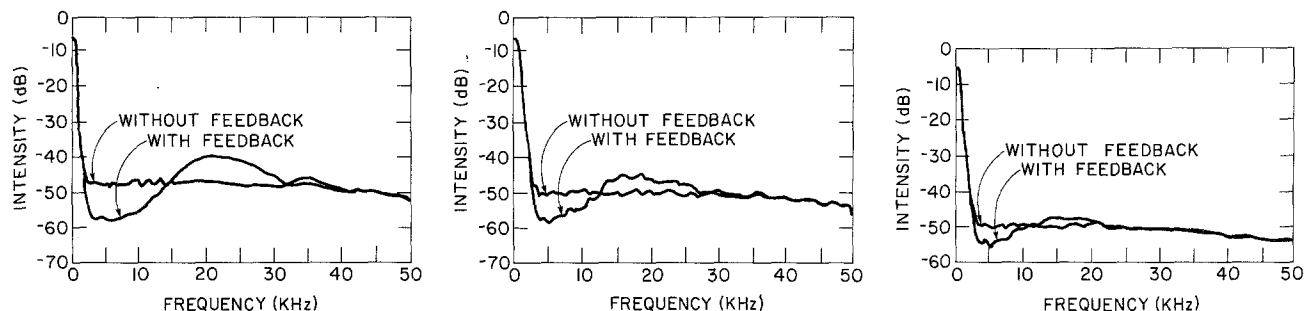


Fig. 6. SHG frequency spectra with and without feedback. From top left corner clockwise, high-frequency cutoffs are 40 kHz, 20 kHz, and 10 kHz for the feedback loop, respectively. Low-frequency cutoff is 3 Hz. The resolution of the spectrum analyzer is 1 kHz

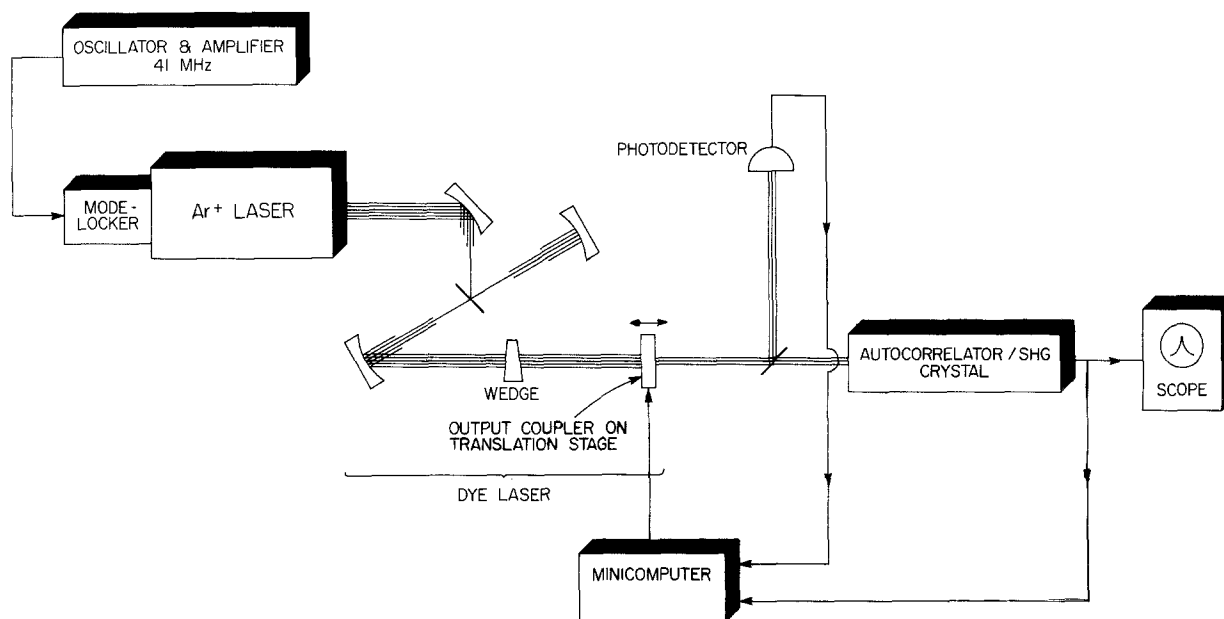


Fig. 7. Schematic of the digital feedback loop

set at 3 Hz to avoid upsetting the phase-lock loop in the HP 8640B oscillator. A few observations are common to all these measurements. First, the noise was lowered by as much as 10 dB up to either the high-frequency cutoff range or 10 kHz, whichever is lower. Unfortunately, all the measurements indicate a concurrent increase of noise at higher frequencies which degrades the pulse width. Attempts to solve this problem by decreasing the bandwidth of the feedback loop or phase compensation at higher frequencies to ensure Nyquist criterion stability failed. The generation of high-frequency noise must be due to nonlinear effects, presumably in the Ar^+ laser system. An overall pulse-width reduction was not observed with the autocorrelator when the analog feedback loop was operative.

The analog loop was unable to operate below 3 Hz due to the need for stability in the phase-lock loop in the Ar^+ laser. In addition, large changes in the mode-locked frequency of the Ar^+ laser could not be made,

since they would affect the power of the Ar^+ laser. For this we used a digital feedback loop.

Figure 7 shows the digital feedback diagram. We first used the autocorrelator to find the best-shaped pulse. Our DEC MINC computer was programmed to find the best pulse shape and measure the pulse width and maximum amplitude of the SHG. The moving arm of the autocorrelator was then fixed at the position of maximum second-harmonic generation; the minicomputer then changed the cavity length to compensate for fluctuations by moving the output coupler of the dye laser, which was mounted on a Klinger translation stage with a $0.5\text{-}\mu\text{m}$ step size.

When the minicomputer first chooses the optimum pulse, there are several possible ways to find the best-shaped (and shortest-duration) pulse. Letting the computer analyze the pulse as a Gaussian curve would require excessive computational time. The method we used was to measure the maximum power and to take its ratio to the power at several points at discrete time

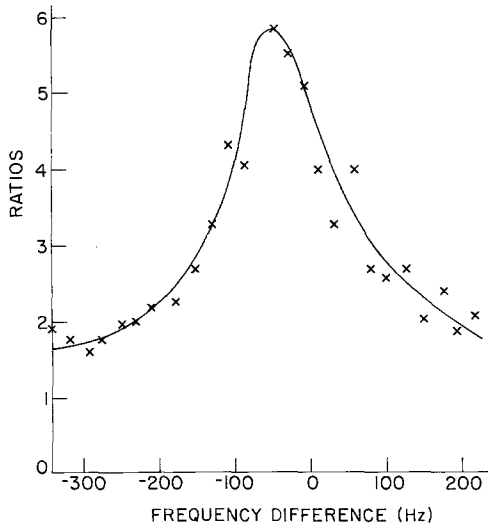


Fig. 8. Graph of ratios between peak SHG power and the power in the wings of the autocorrelated pulse that result with the second dye laser in a function of frequency difference. Best pulse results are at -50 Hz. The zero frequency is the position of the maximum SHG output

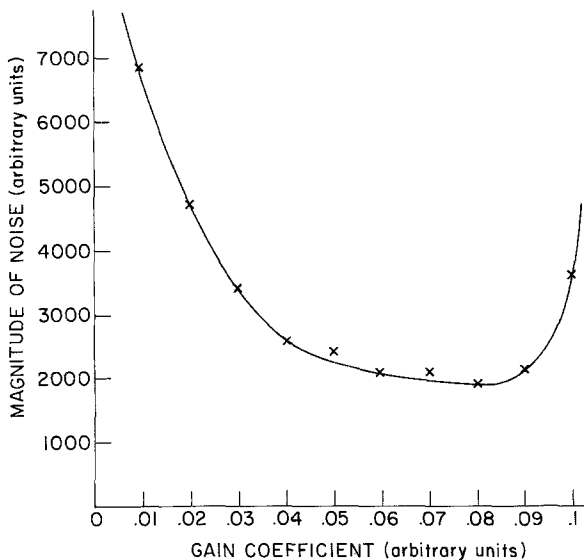


Fig. 9. Root-mean-squared value of the noise of the SHG as a function of the gain coefficient of the digital loop. Oscillation occurs when gain coefficient is greater than 0.09

delays from the maximum. This method distinguishes properly formed pulses from those of insufficient power. Figure 8 shows these ratios as a function of frequency, which peaks sharply at 50 Hz below the frequency of maximum second-harmonic generation. While this method is not guaranteed to find the best pulse, the results of many experiments leave us confident that the results are close to optimum.

The noise from the SHG was filtered through a 20-Hz low-pass filter to take into account the speed limit of the computer and the translation stage. While this was

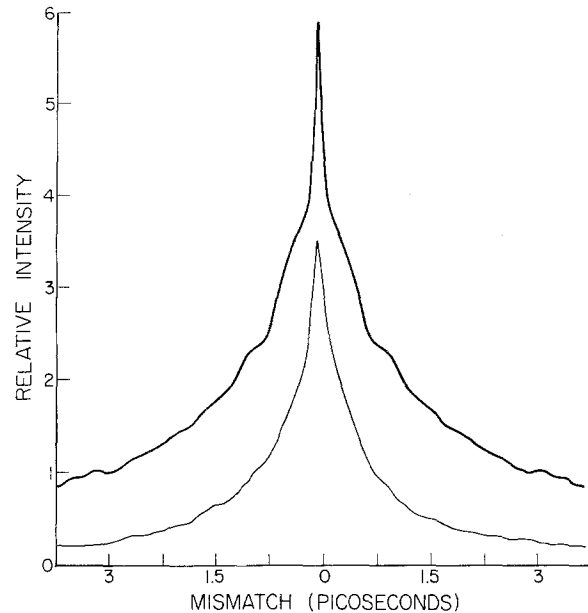


Fig. 10. Autocorrelation traces with and without the digital feedback. Top trace represents the pulse that results after one hour of drift without feedback; a pulse width of 2.2 ps with an autocorrelation spike is measured. Bottom trace is the pulse that results after one hour with feedback. Pulse width of 0.7 ps is measured

only a minute portion of the noise spectrum, measurements with a higher frequency cutoff have given similar results.

Figure 9 shows the magnitude of the noise as the gain coefficient in the loop was changed. The gain loop times the magnitude of the noise determines the number of $0.5\text{-}\mu\text{m}$ steps that the translation stage takes. As the gain coefficient increases, the amount of noise decreases with an improvement of approximately 6 dB up to the point where oscillation begins.

Our digital loop was particularly successful in eliminating long-term drift in our system. Figure 10 compares the pulse-feedback technique with the pulse resulting from one hour of drift. In the latter case, the initial pulse width of 0.7 ps has changed to a pulse width of 2.2 ps.

There are several limitations to the achievable frequency response of the feedback. The basic system on the computer has a maximum response speed of 40 Hz with the programs used. While the RT 11 system on the DEC MINC computer could increase the feedback time, the 400-Hz response of the translation stage provides an upper limit to possible reaction time. Nevertheless, the digital feedback allowed the stabilization of our system at the shortest pulse setting over long time periods [14]. Moreover, the cavity length was adjusted in increments of half-micron steps with the translation stage, which gives greater accuracy than that attainable when a quartz or Invar rod is used for length stabilization.

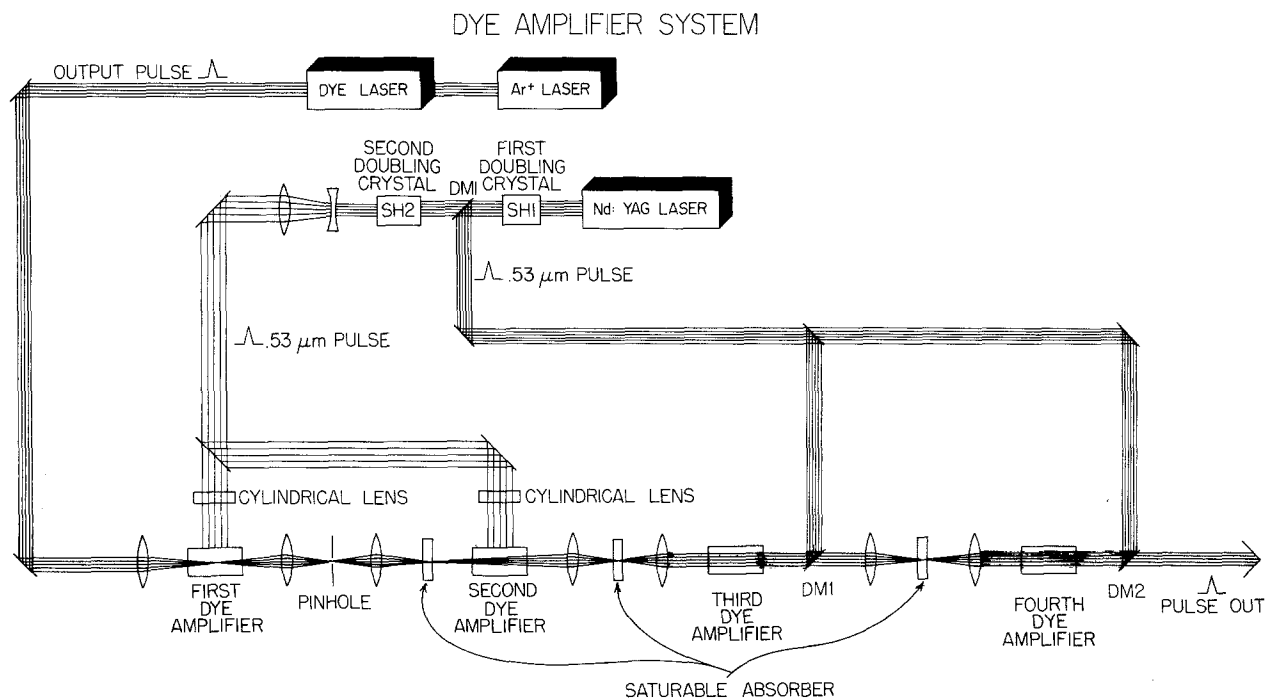


Fig. 11. Schematic of the dye amplifier system. DM1 and DM2 are dichroic mirrors

4. The Dye Amplifier

A dye-laser amplifier was constructed to amplify the picosecond pulses generated by the synchronously pumped, mode-locked dye-laser system. The amplifier system is similar to that reported by Migus et al. [15]. In our system, the amplifier chain consists of four separate stages which enable us to obtain extremely high gain as well as to control the amplified spontaneous emission (ASE) effectively.

Figure 11 is a schematic of the dye amplifier. The pulse train from the sync-pumped Rhodamine 6G cw dye laser consists of pulses, typically about one picosecond wide, which are separated by about 12 ns. The pumping source for the amplifier is the second-harmonic output of a Q-switched Nd:YAG laser, giving pulses about 10 ns long at a 10-Hz repetition rate. In our system, two crystals are used to double the frequency of the output of the Nd:YAG laser at $1.06 \mu\text{m}$. The second-harmonic output at a wavelength of 530 nm is generated by the two crystals, SH1 and SH2, which have power levels of approximately 120 mJ and 14 mJ at their respective outputs.

Twenty percent of the output of the second crystal pumps the first stage and the remaining 80% is used for the second stage. The first two stages contain identical 2-cm-long dye cells [16]. The windows of the cell are at the Brewster angle to minimize the reflection of the incoming beam and to eliminate the possibility of optical feedback.

Since gain saturation can broaden the width of the picosecond laser pulse, it is highly undesirable. One technique to control such saturation is by expanding the laser-beam diameter before each stage. Furthermore, proper choice of dye concentrations also greatly affects the performance of the amplifier. It must be adjusted so that the length of the penetration depth of the pump overlaps with the beam diameter inside the dye cell. Finally, the choice of the dyes is selected such that the emission cross sections of the dye at the wavelength of the incoming beam and at the chosen concentration are excellent.

In our system, we use a beam diameter of $200 \mu\text{m}$ inside the first dye cell and 1 mm inside the second cell. The first stage contains Kiton Red ($3 \times 10^{-4} \text{ M}$) while the second stage uses Rhodamine 640 (10^{-4} M). The first stage also consists of a pinhole ($100 \mu\text{m}$) and a saturable absorber. The pinhole is used to reduce the amount of ASE going into the second dye cell. The saturable absorber provides an additional optical isolation between the second and first stages and reshapes the amplified picosecond dye-laser pulses. Cresyl violet is used, and the concentration is adjusted such that the ASE is attenuated by a factor of three, while the amplified pulses suffer only 10% loss. The third dye cell [5 cm long with Rhodamine 640 ($3 \times 10^{-5} \text{ M}$)] is pumped longitudinally for better beam quality by 20% of the output of the first crystal. The last stage, which contains a 10-cm-long cell (Rhodamine 640 at

10^{-5} M), is also pumped longitudinally by the remainder of the output of the first crystal. The beam diameter of the dye laser is expanded to 3 mm and 6 mm inside the third and last stages, respectively. Saturable absorbers (Malachite Green) are again used to control the ASE and the leading edge of the picosecond pulses between these stages.

In order to achieve amplification, the Nd:YAG laser must be phase-locked with the dye laser. This is done by counting down the 41-MHz electronic signal generated by the mode-locker driver to a 10-Hz signal which is then used to trigger both the flash lamps and the Q-switch inside the Nd:YAG laser. Time jitter of less than 2 ns between the dye pulse and the Nd:YAG pulse is achieved and is good enough to maintain proper amplification.

Typically, output laser energies of about 2 mJ with about 1-ps pulses at a repetition rate of 10 Hz are achieved. Overall system gain is about 3×10^6 , a result comparable to that obtained elsewhere [15]. A picosecond spectral continuum can be generated by focusing the amplified picosecond pulses into water. This continuum could be generated extending from the infrared to the ultraviolet.

Conclusions

In this paper, we have described a sync-pumped system for producing picosecond pulses. Pulses of 0.7-ps duration have been achieved. An analog and a digital feedback loop for our sync-pump system stabilized the pulse width of our picosecond pulses and significantly lowered the noise up to 10 kHz by 10 dB. The limitation of the analog system was the 10-kHz response time of the mode locker while the digital loop was limited by the computer and translation-stage speeds.

Several interesting experiments can now be performed with our sync-pump system. First, our feedback system

would be improved if we could increase the response time of our system to approximately 200 kHz, since a large amount of noise originating from both the dye jet and the argon-ion plasma has frequency components centered around 100–150 kHz. A piezo-electric transducer in a feedback loop connected to the output coupler of the dye laser may succeed in reducing this high-frequency noise. Moreover, new methods of stabilizing the Ar⁺ plasma should be studied. The extension of this method could have the same impact on time-domain spectroscopy as the development of ultranarrow frequency-tunable lasers on atomic and molecular-resonance spectroscopy.

References

1. *Picosecond Phenomena II*, ed. by R.M.Hochstrasser, W.Kaiser and C.V.Shank, Springer Sec. Chem. Phys. **14** (Springer, Berlin, Heidelberg New York 1980)
2. C.V.Shank, R.L.Fork, R.F.Leheny, J.Shah: Phys. Rev. Lett. **42**, 112 (1979)
3. P.Liu, W.L.Smith, H.Lotem, J.H.Bechtel, N.Bloembergen: Phys. Rev. B **17**, 4620 (1978)
4. C.K.Chan, S.O.Sari: Appl. Phys. Lett. **25**, 403 (1974)
5. R.L.Fork, B.I.Greene, C.V.Shank: Appl. Phys. Lett. **38**, 671 (1981)
6. J.P.Heritage, R.K.Jain: Appl. Phys. Lett. **32**, 101 (1978)
7. R.K.Jain, C.P.Ausschnitt: Opt. Lett. **2**, 117 (1978)
8. J.deVries, D.Bebelaar, J.Langelaar: Opt. Commun. **18**, 24 (1976)
9. C.P.Ausschnitt, R.K.Jain, J.P.Heritage: IEEE J. QE **15**, 912 (1979)
10. R.K.Jain, J.P.Heritage: Appl. Phys. Lett. **32**, 41 (1978)
11. A.Scavennec: Opt. Commun. **17**, 14 (1976)
12. R.L.Fork, F.A.Beisser: Appl. Opt. **17**, 3534 (1978)
13. C.V.Shank, E.P.Ippen: Appl. Phys. Lett. **24**, 373 (1974)
14. S.R.Rotman, C.B.Roxlo, D.Bebelaar, M.M.Salour: Appl. Phys. Lett. **36**, 886 (1980)
15. A.Migus, C.V.Shank, E.P.Ippen, R.L.Fork: IEEE J. QE-**18**, 101 (1982)
16. P.Drell, S.Chu: Opt. Commun. **28**, 343 (1979), M.M.Salour: Opt. Commun. **22**, 202 (1977)